Water Oxidation

DOI: 10.1002/anie.201307509

A Self-Improved Water-Oxidation Catalyst: Is One Site Really Enough?**

Isidoro López, Mehmed Z. Ertem, Somnath Maji, Jordi Benet-Buchholz, Anke Keidel, Uwe Kuhlmann, Peter Hildebrandt, Christopher J. Cramer, Victor S. Batista,* and Antoni Llobet**

Abstract: *The homogeneous catalysis of water oxidation by transition-metal complexes has experienced spectacular development over the last five years. Practical energy-conversion schemes, however, require robust catalysts with large turnover frequencies. Herein we introduce a new oxidatively rugged and powerful dinuclear water-oxidation catalyst that is generated by self-assembly from a mononuclear catalyst during the catalytic process. Our kinetic and DFT computational analysis shows that two interconnected catalytic cycles coexist while the mononuclear system is slowly and irreversibly converted into the more stable dinuclear system: an extremely robust water-oxidation catalyst that does not decompose over extended periods of time.*

The replacement of fossil fuels by green and renewable solar-energy carriers is one of the most important challenges our society is facing today.[1] Intense research is currently being devoted to this topic, with emphasis on the development and characterization of new catalysts for water splitting, such as the dinuclear Ru complexes introduced herein.

Nature has been using sunlight to oxidize water and generate carbohydrates (solar fuels) in photosynthesis for over 2.5 billion years.[2] Artificial systems inspired by nature have been designed to capture solar light and extract protons and electrons from water to generate useful chemical fuels. Therefore, mastering and understanding water-oxidation catalysis is one of the key elements needed for this strategy to succeed. Although this research field is becoming extremely active,[3] significant advances are still needed to develop a sufficiently rugged and efficient water-oxidation catalyst that will be useful in large-scale practical applications.

Since the discovery by Zong and Thummel that even mononuclear Ru complexes were active as water-oxidation catalysts (WOCs),[4] there has been substantial development of such complexes.[5] Several catalysts have been identified, and considerable knowledge with respect to their activity has been gathered.[6] From a mechanistic perspective, Meyer and co-workers have offered a description of water oxidation at the molecular level.[7] Specifically, they proposed that O–O bond formation takes place through water nucleophilic attack (WNA) on a highly oxidized metal–oxo complex, as shown in a simplified manner on the left side of Scheme 1.

Catalysts such as $[Ru(trpy)(bpym)(H_2O)]^{2+}$ (trpy is 2,2′:6′,2″-terpyridine, bpym is 2,2′-bipyrimidine)[8] have been reported to have impressive turnover numbers in excess of 28000. Nevertheless, *practical* applications will require catalysts with turnover numbers that are at least a few orders of magnitude higher. For the design of such highly efficient water-oxidation catalysts, it is of paramount importance to understand the pathways that lead to oxygen evolution from water and also the different reactions coupled to the catalytic cycle that might drive intermediate species towards unproductive pathways and decomposition. Furthermore, the discovery of pathways that couple to other beneficial parallel catalytic cycles would be particularly valuable.

Herein we report the synthesis and characterization of new dinuclear Ru complexes of the general formula $[(trpy)(5,5'\text{-}X_2\text{-}bpy)Ru^{IV}(\mu\text{-}O)Ru^{IV}(trpy)(O)(H_2O)]^{4+}$ (bpy is 2,2′-bipyridine; X = H for $\mathbf{1}^{4+}$ and X = F for $\mathbf{2}^{4+}$) that are highly efficient and very robust WOCs. We found that these complexes are generated from their corresponding mononuclear WOC counterparts $[Ru(trpy)(5,5'\text{-}X_2\text{-}bpy)(H_2O)]^{2+}$ (X = H: $\mathbf{4}^{2+}$; X = F: $\mathbf{5}^{2+}$).[9] The addition of $[Ru^{VI}(trpy)(O)_2(H_2O)]^{2+}$ ($\mathbf{3}^{2+}$) to $\mathbf{4}^{2+}$ or $\mathbf{5}^{2+}$ in the presence of Ce^{IV} under acidic conditions generates complex $\mathbf{1}^{4+}$ or $\mathbf{2}^{4+}$, respectively, as indicated in Equation (1) (in the structures, the trpy ligand

[*] I. López, Dr. S. Maji, Dr. J. Benet-Buchholz, Prof. A. Llobet
Institute of Chemical Research of Catalonia (ICIQ)
Av. Països Catalans 16, 43007 Tarragona (Spain)
E-mail: allobet@iciq.cat
A. Keidel, Dr. U. Kuhlmann, Prof. P. Hildebrandt
Technische Universität Berlin, Institut für Chemie
Sekr. PC14, Strasse des 17. Juni 135, 10623 Berlin (Germany)
Dr. M. Z. Ertem
Department of Chemistry, Brookhaven National Laboratory
Building 555A, Upton, NY 11973 (USA)
Dr. M. Z. Ertem, Prof. V. S. Batista
Department of Chemistry, Yale University
P.O. Box 208107, New Haven, CT 06520-8107 (USA)
Prof. C. J. Cramer
Department of Chemistry, Chemical Theory Center, and
Supercomputing Institute, University of Minnesota
207 Pleasant Street SE, Minneapolis, MN 55455-0431 (USA)

[**] Support from MINECO (CTQ2010–21497 and PRI-PIBIN-2011-1278), an FPU grant to I.L., and a Torres Quevedo contract to S.M. are gratefully acknowledged. Support has also been received from the Cluster of Excellence (UniCat) and the US Department of Energy (DOE) (Grant DE-SC0001423 to V.S.B.). M.Z.E. received funding from a Computational Materials and Chemical Sciences (CMCSN) project at Brookhaven National Laboratory under contract DE-AC02-98CH10886 with the US DOE and was supported by its Division of Chemical Sciences, Geosciences and Biosciences, Office of Basic Energy Sciences. C.J.C. acknowledges support from the US National Science Foundation (CHE-0952054).

Supporting information for this article is available on the WWW under http://dx.doi.org/10.1002/anie.201307509.

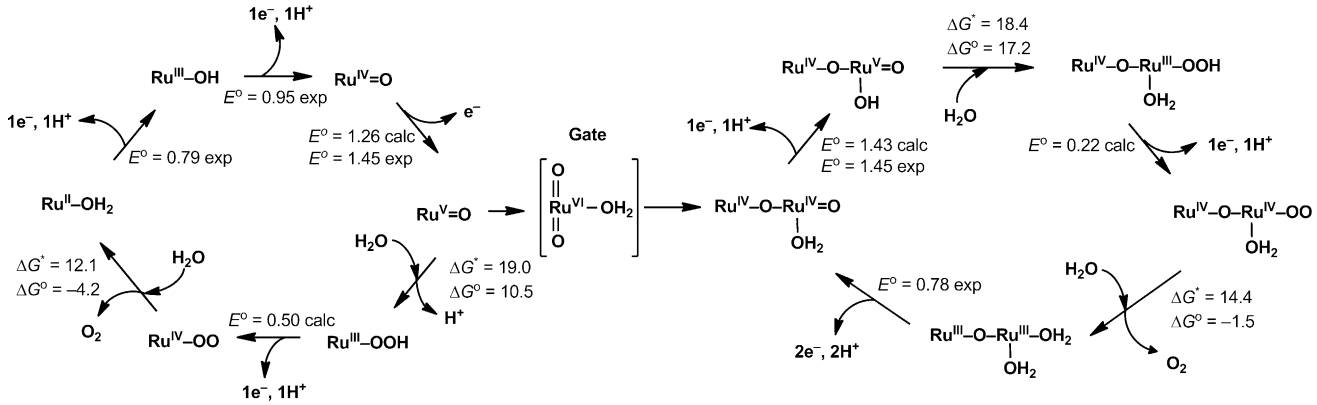

Scheme 1. Proposed interconnection of catalytic schemes for mononuclear (left) and dinuclear (right) Ru complexes (polypyridyl ligands are not shown). Energies are reported in kcal mol^{-1}, and redox potentials are reported in V vs. the SSCE reference electrode at pH 1.0. DFT calculations at the M06-L level of theory (calc) are compared to experiments (exp).

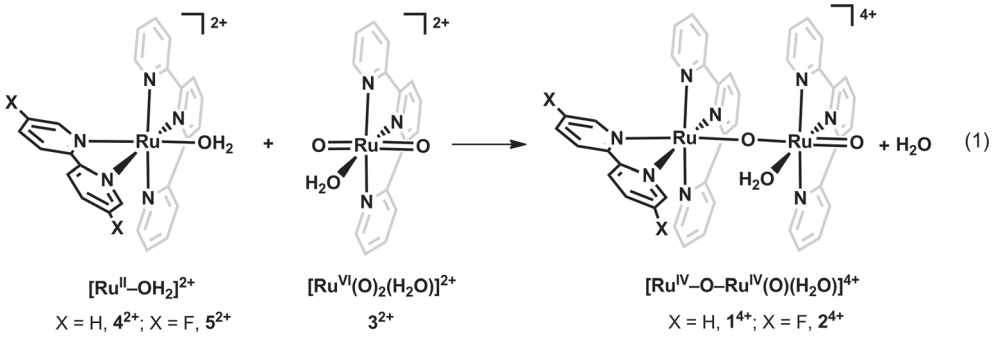

backbone is drawn in gray to indicate that is situated at the back; polypyridyl ligands are omitted in the formulas).

Complexes $\mathbf{1}^{4+}$ and $\mathbf{2}^{4+}$ were thoroughly characterized by analytical, spectroscopic, and electrochemical techniques. The X-ray crystal structures of $\mathbf{1}^{4+}$ and $\mathbf{2}^{4+}$ were solved by means of single-crystal XRD (see Figure 1 for $\mathbf{1}^{4+}$ and the Supporting Information for $\mathbf{2}^{4+}$). The short Ru–O distance (1.747 Å) in $\mathbf{1}^{4+}$ falls in the lower range of values reported for

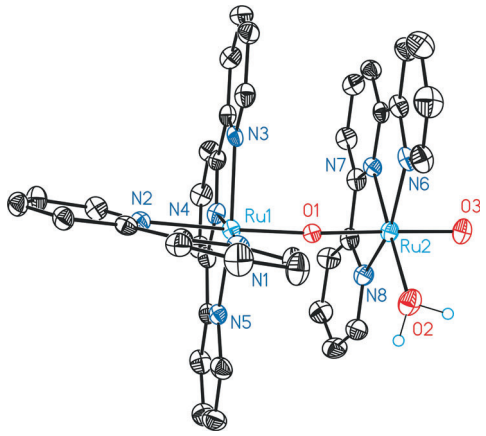

Figure 1. ORTEP plot (ellipsoids drawn at 50% probability) of the X-ray crystal structure of $\mathbf{1}^{4+}$ (Ru cyan, O red, N blue, C black). H atoms are not shown except for the aqua ligand, in which they are represented as small light-blue circles.

Ru^{IV}=O groups.[10] In contrast, the Ru–O distance for the Ru^{IV}–OH$_2$ group of the same metal center is 2.120 Å. Notably, the Ru-O-Ru angle (176.1°) is nearly linear. Complexes $\mathbf{1}^{4+}$ and $\mathbf{2}^{4+}$ are diamagnetic, as expected for high-field μ-oxo dinuclear d^4 Ru complexes (see the Supporting Information for their NMR spectra).[11]

Complexes $\mathbf{1}^{4+}$ and $\mathbf{2}^{4+}$ both have a very strong vibrational band at 801 cm^{-1}, as shown in the resonance Raman (rR) spectrum for $\mathbf{2}^{4+}$ (Figure 2). We assign this band as the Ru=O stretching mode. Labeling experiments with $H_2{}^{18}O$ led to a redshift of this mode to 760 cm^{-1}, which corresponds to an isotopic shift of 41 cm^{-1}. Mixed labeling with a 1:1 $H_2{}^{16}O$/$H_2{}^{18}O$ mixture did not generate any new modes in the rR spectrum; this result is consistent with a terminal Ru=O bond. The frequency of this mode is in agreement with related Ru=O complexes reported previously.[10e,12] A very interesting feature of the rR spectrum is the presence of small bands at 727, 714, 700, and 675 cm^{-1} that can be used as a fingerprint for the identification of this complex.

The electrochemistry of complexes $\mathbf{1}^{4+}$ and $\mathbf{2}^{4+}$ was examined in 0.1 M triflic acid by means of cyclic voltammetry (CV), differential pulse voltammetry (DPV), and coulometry (Figure 3; see also the Supporting Information). Complex $\mathbf{1}^{4+}$ underwent a two-electron reduction, as confirmed by coulometry, from the formal oxidation state IV,IV to III,III, in association with two proton-transfer steps, according to Equation (2) (polypyridyl ligands not shown; SSCE = sodium saturated calomel electrode):

$$[Ru^{IV}-O-Ru^{IV}(O)(H_2O)]^{4+} + 2e^- + 2H^+ \rightarrow [Ru^{III}-O-Ru^{III}(H_2O)_2]^{4+} \qquad E^\circ = 0.78\ V \text{ vs. SSCE} \tag{2}$$

On the anodic part of the voltammogram, a further electron-transfer process was observed together with a large

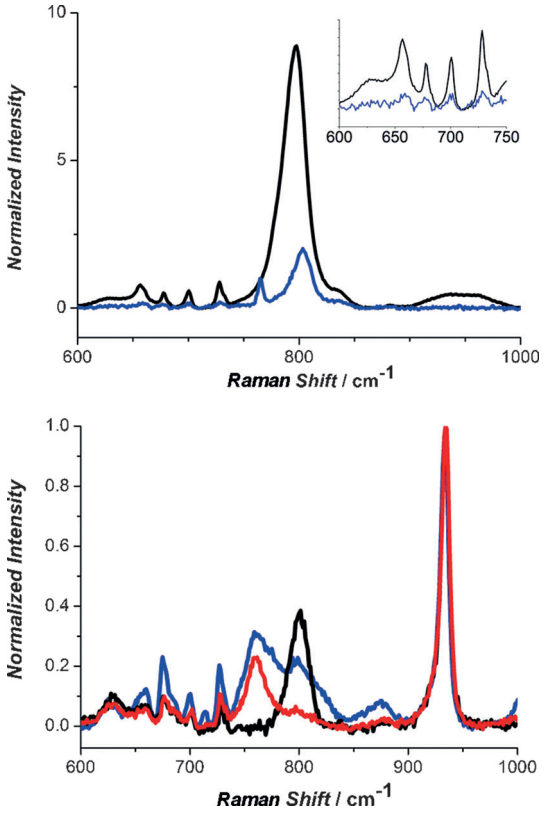

Figure 2. Top: Overlay of the rR spectra of $\mathbf{2}^{4+}$ (black) and the reaction product obtained after the addition of Ce^{IV} (3 equiv) to complex $\mathbf{5}^{2+}$ (blue). Both spectra were recorded in 0.1 M triflic acid in $H_2{}^{16}O$. The inset shows an enlargement of the fingerprint region mentioned in the main text. Bottom: Overlay of rR spectra obtained after the treatment of complex $\mathbf{5}^{2+}$ with Ce^{IV} (3 equiv) in 0.1 M $HClO_4$ in $H_2{}^{16}O$ (black), $H_2{}^{18}O$ (red), and $H_2{}^{16}O/H_2{}^{18}O$ (1:1; blue). Further experimental details are given in the Supporting Information.

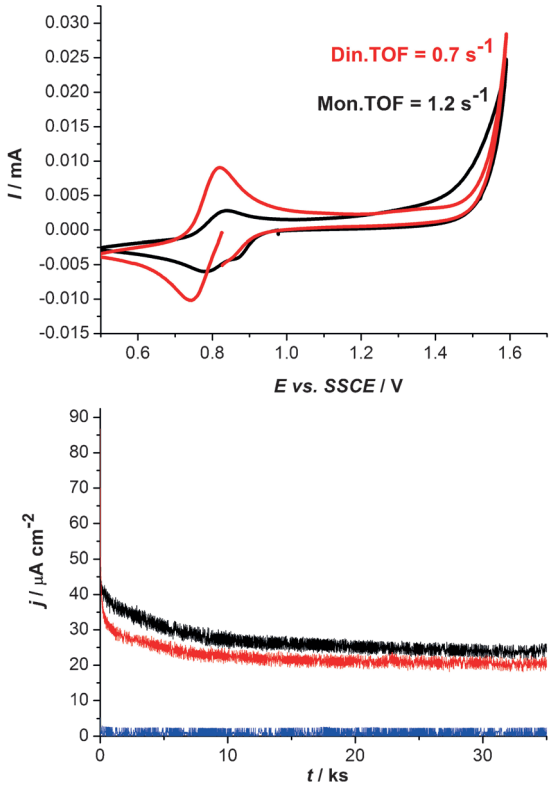

Figure 3. Top: CV of 0.5 mM solutions of $\mathbf{1}^{4+}$ (red) and $\mathbf{4}^{2+}$ (black) in 0.1 M triflic acid (pH 1.0) with a polished glassy-carbon working electrode, a platinum-wire counter electrode, and Hg/Hg_2SO_4, K_2SO_4 (sat.) as the reference electrode (potentials reported vs. SSCE). "Din." stands for the dinuclear catalyst, "Mon." for the mononuclear catalyst. Bottom: Controlled-potential electrolysis at 1.6 V vs. SSCE of 0.4 mM solutions of complexes $\mathbf{4}^{2+}$ (black) and $\mathbf{1}^{4+}$ (red) in 0.1 M triflic acid. The results of a blank experiment without a catalyst are also shown (blue). An activated boron-doped diamond disk (3 mm diameter) was used as the working electrode, platinum wire as the counter electrode, and Hg/Hg_2SO_4, K_2SO_4 (sat.) as the reference electrode (potentials were converted to values vs. SSCE).

current intensity and attributed to the electrocatalytic oxidation of water to dioxygen. A one-electron process that generates a very reactive species responsible for O–O bond formation [Eqs. (3) and (4)] is proposed, followed by a sequence of reactions leading to dioxygen formation (Scheme 1, right side).

$$[Ru^{IV}\text{–}O\text{–}Ru^{V}(O)(OH)]^{4+} + 1\,e^- + 1\,H^+ \rightarrow [Ru^{IV}\text{–}O\text{–}Ru^{IV}(O)(H_2O)]^{4+} \qquad E_{onset} = 1.45\ V\ vs.\ SSCE \tag{3}$$

$$[Ru^{IV}\text{–}O\text{–}Ru^{V}(O)(OH)]^{4+} + H_2O \rightarrow [Ru^{IV}\text{–}O\text{–}Ru^{III}(OOH)(OH_2)]^{4+} \tag{4}$$

Formal oxidation states are indicated to facilitate electron counting even though it is well-known that the oxo bridge promotes charge-transfer interactions between the Ru metal centers.[13] DFT calculations carried out at the M06-L[14] level of theory (see the Supporting Information for details) to characterize the reaction intermediates as well as the transition states provided a complete catalytic cycle for the dinuclear $\mathbf{1}^{4+}$ complex and also for the mononuclear $\mathbf{4}^{2+}$ complex for comparative purposes (Scheme 1). The O–O bond-formation step through WNA on $[Ru^{IV}\text{–}O\text{–}Ru^{V}(O)(OH)]^{4+}$ [Eq. (4)] was found to be the rate-determining step of the catalytic cycle with a $\Delta G^{\ddagger}$ value of 18.4 kcal mol^{-1}. The optimized transition-state structure features a water molecule which forms the O–O bond with concomitant transfer of a proton to the neighboring Ru–OH group (Figure 4, left) to generate the corresponding hydroperoxo complex, $[Ru^{IV}\text{–}O\text{–}Ru^{III}(OOH)(OH_2)]^{4+}$.

The next step corresponds to a proton-coupled electron transfer with a very low redox potential and leads to the formation of a superoxo intermediate,

$$[Ru^{IV}\text{–}O\text{–}Ru^{III}(OOH)(OH_2)]^{4+} - 1\,e^- - 1\,H^+ \rightarrow [Ru^{IV}\text{–}O\text{–}Ru^{IV}(OO)(OH_2)]^{4+} \qquad E^{\circ} = 0.22\ V \tag{5}$$

which subsequently evolves O_2 (Figure 4, right) and generates the III,III complex,

$$[Ru^{IV}\text{–}O\text{–}Ru^{IV}(OO)(OH_2)]^{4+} + H_2O \rightarrow [Ru^{III}\text{–}O\text{–}Ru^{III}(OH_2)_2]^{4+} + O_2 \tag{6}$$

thus closing the catalytic cycle. For the mononuclear complex $\mathbf{4}^{2+}$, the $\Delta G^{\ddagger}$ value for the WNA step is 19.0 kcal mol^{-1}, which

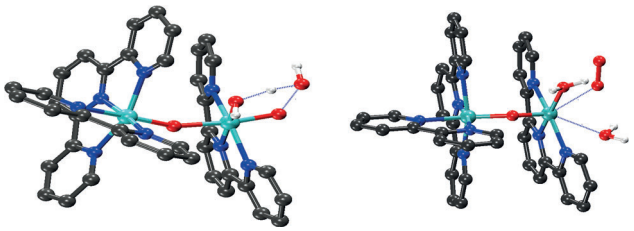

Figure 4. Ball-and-stick representation of the optimized transition-state structures for the O–O bond-formation (left) and O_2-evolution steps (right). H atoms are shown only for the aqua and hydroxy ligands.

is very similar to that for the corresponding dinuclear complex $\mathbf{1}^{4+}$ (see Scheme S2 in the Supporting Information for the detailed mechanism).

From the electrochemical experiments described in Figure 3, turnover frequencies (TOFs) of 0.7 s^{-1} for $\mathbf{1}^{4+}$ and 1.2 s^{-1} for $\mathbf{4}^{2+}$ were calculated;[15] these TOFs are comparable to reported values for mononuclear complexes.[8,9,16] The capacity of $\mathbf{1}^{4+}$ to act as a WOC was also tested electrochemically under a constant applied potential. We performed potentiometric experiments for both $\mathbf{1}^{4+}$ and $\mathbf{4}^{2+}$ to evaluate their relative performance at longer time scales (Figure 3). At an applied potential of 1.6 V vs. SSCE, initial current densities of approximately 40 μA cm^{-2} were reached for $\mathbf{1}^{4+}$ and $\mathbf{4}^{2+}$. For $\mathbf{1}^{4+}$, the current density decreased to 20 μA at about 10 ks and remained constant thereafter. By contrast, for $\mathbf{4}^{2+}$ the current slowly dropped over time until it merged with that of $\mathbf{1}^{4+}$ at approximately 30 ks. This phenomenon is attributed to the slow but progressive and irreversible conversion of the mononuclear complex $\mathbf{4}^{2+}$ into the corresponding dinuclear complex $\mathbf{1}^{4+}$, as proposed in Scheme 1 and as demonstrated by UV/Vis and rR spectroscopy (see below). At 35 ks, turnover numbers of 14930 and 6683 were estimated for $\mathbf{4}^{2+}$ and $\mathbf{1}^{4+}$, respectively.

The bulk electrolysis experiment at $E_{app} = 1.4$ V was also followed spectrophotometrically by UV/Vis absorption spectroscopy (Figure 5). Interestingly, the absorption bands of $\mathbf{1}^{4+}$, found at 457 and 690 nm, started to emerge as catalysis proceeded. After the application of a constant potential for 2 days, 23% conversion of $\mathbf{4}^{2+} \rightarrow \mathbf{1}^{4+}$ was observed. This mononuclear-to-dinuclear conversion could also be observed in the rR spectra at very early stages of the water-oxidation reaction upon the addition of Ce^{IV} (3 equiv) to $\mathbf{5}^{2+}$ (Figure 2). Indeed, shortly after the addition of Ce^{IV}, the rR spectrum displayed a highly intense band at 801 cm^{-1} and four weaker bands at 727, 714, 700, and 675 cm^{-1} characteristic of $\mathbf{2}^{4+}$. In sharp contrast, the exposure of $\mathbf{1}^{4+}$ or $\mathbf{2}^{4+}$ for long periods of time to the same conditions (35 ks at 1.6 V vs. SSCE) did not lead to any change in the UV/Vis spectrum. This result illustrates the ruggedness of $\mathbf{1}^{4+}$ as a water-oxidation catalyst that does not exhibit any sign of fatigue even after controlled-potential electrolysis at 1.6 V vs. SSCE for 35 ks.

These experiments manifest the interconnection of the two catalytic cycles for the mononuclear $\mathbf{4}^{2+}$ and dinuclear $\mathbf{1}^{4+}$ species. The link between the two catalytic cycles is essentially $[Ru^{VI}(trpy)(O)_2(H_2O)]^{2+}$ ($\mathbf{3}^{2+}$), which can be generated by the loss of bpy from the mononuclear complex, potentially at oxidation state V:

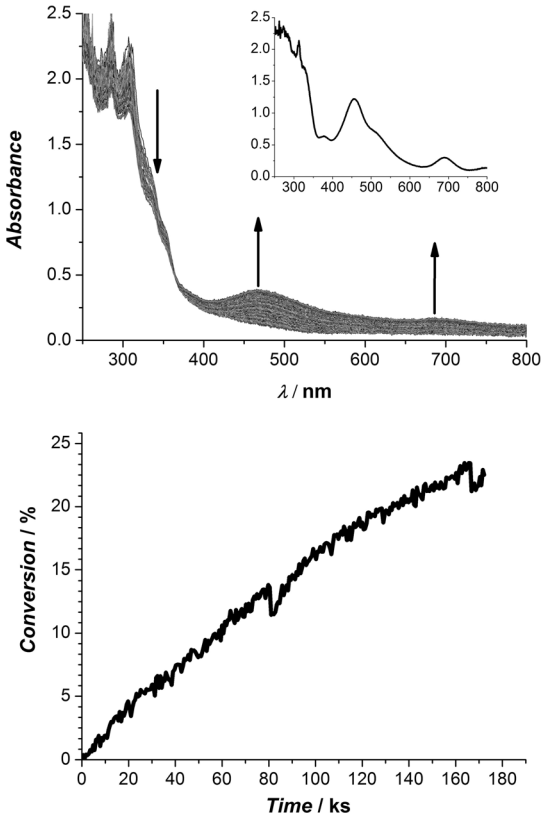

Figure 5. Top: UV/Vis absorption spectra monitoring the controlled-potential electrolysis of a 0.5 mM solution of $\mathbf{4}^{2+}$ in 0.1 M HOTf for 2 days at 1.4 V vs. SSCE with a platinum-mesh working electrode, a platinum-wire counter electrode, and a Ag/AgCl, NaCl (3 M) reference electrode. Spectra were recorded every 10 min. Inset: UV/Vis spectrum of $\mathbf{1}^{4+}$ in 0.1 M HOTf. Right: Conversion of mononuclear $\mathbf{4}^{2+}$ into dinuclear $\mathbf{1}^{4+}$ over time, as based on absorbance change at 460 nm.

$$[(trpy)(bpy)Ru^{V}{=}O]^{3+} + Ce^{IV} + 2\,H_2O \rightarrow \textit{trans}\text{-}[(trpy)Ru^{VI}(O)_2(H_2O)]^{2+} + bpyH^{+} + H^{+} + Ce^{III} \quad (7)$$

The strong *trans* effect of the $Ru^{V}{=}O$ group produces a weakening of one of the Ru–N bpy bonds that eventually leads to the loss of the bpy ligand. Furthermore, the *trans*-$Ru(O)_2$ entity is known to generate very stable complexes[17] and thus is an additional driving force for the loss of bpy. Once the bpy ligand is released, the reaction of $\mathbf{3}^{2+}$ with $\mathbf{4}^{2+}$ [Eq. (1)] constitutes the entry into the dinuclear catalytic cycle. The free-energy values obtained at the M06-L level of theory indicate that the proposed interconversion pathway is feasible (see Scheme S3 in the Supporting Information) and further support this hypothesis. This interconversion process also occurs between $\mathbf{5}^{2+}$ and $\mathbf{2}^{4+}$, thus suggesting a general interconversion process of single-site catalysts. These findings shed light on the in situ generation of long-lasting water-oxidation catalysts based on dinuclear complexes.

The greater stability of the dinuclear complexes can be attributed to a number of factors. First, the presence of two Ru centers that are electronically coupled through an oxo bridge allows for fast intramolecular electron transfer (ET) within the species generated in the catalytic cycle. Thus, with the involvement of two metal centers, the burden of multiple

electron-transfer steps at a single site is overcome. Second, the presence of spatially separated, nonsymmetrical Ru centers enables fine-tuning of each site, that is, the optimization of one site for electron relay and the other site for proton-coupled ET, which is responsible for the primary interaction with the water molecules. Third, the *trans*-dioxo geometry at higher oxidation states stabilizes the dinuclear complex as opposed to the mononuclear $\mathbf{3}^{2+}$, which is not an active water-oxidation catalyst. Furthermore, the higher oxidation states of mononuclear monoaqua Ru complexes lead to ligand loss and subsequent decomposition. Finally, the oxo bridge and the terminal Ru=O group can act as anchors for hydrogen bonding if required, as nicely illustrated in the transition-state structure depicted in Figure 4. This hydrogen bonding has been shown previously to be crucial for reducing the activation energy of transition states.[18]

In summary, we have shown that WOCs based on mononuclear monoaqua Ru complexes can be slowly converted into active dinuclear catalysts through a self-assembly type of process. These dinuclear complexes are much more robust than the mononuclear precursors and exhibit similar activity as WOCs. Thus, we have shown for the first time that two interconnected catalytic cycles coexist, whereby the mononuclear catalytic system is slowly and irreversibly converted into the more stable dinuclear catalytic system. We have further characterized the catalytic cycle on the basis of DFT calculations, which provided very good agreement with experimental observations and rationalize the overall mechanism in microscopic detail.

Received: August 26, 2013
Revised: October 25, 2013
Published online: November 20, 2013

Keywords: density functional calculations · reaction mechanisms · resonance Raman spectroscopy · ruthenium electrochemistry · water-oxidation catalysis

[1] A. Melis, *Energy Environ. Sci.* **2012**, *5*, 5531.
[2] a) J. Barber, *Philos. Trans. R. Soc. London Ser. A* **2007**, *365*, 1007 – 1023; b) J. Raymond, R. E. Blankenship, *Coord. Chem. Rev.* **2008**, *252*, 377 – 383; c) B. Patel, B. Tamburic, F. W. Zemichael, P. Dechatiwongse, K. Hellgardt, ISRN Renewable Energy 2012, **2012**, 14.
[3] R. Bofill, J. García-Antón, L. Escriche, X. Sala, A. Llobet in *Comprehensive Inorganic Chemistry II, Coordination and Organometallic Chemistry, Vol. 8* (Ed.: W. W. Y. Vivian), Elsevier Limited, Oxford, **2012**.
[4] R. Zong, R. P. Thummel, *J. Am. Chem. Soc.* **2005**, *127*, 12802 – 12803.
[5] a) J. J. Concepcion, J. W. Jurss, J. L. Templeton, T. J. Meyer, *J. Am. Chem. Soc.* **2008**, *130*, 16462 – 16463; b) D. J. Wasylenko, C. Ganesamoorthy, B. D. Koivisto, M. A. Henderson, C. P. Berlinguette, *Inorg. Chem.* **2010**, *49*, 2202 – 2209; c) L. Duan, A. Fischer, Y. Xu, L. Sun, *J. Am. Chem. Soc.* **2009**, *131*, 10397 – 10399; d) J. L. Boyer, D. E. Polyansky, D. J. Szalda, R. Zong, R. P. Thummel, E. Fujita, *Angew. Chem.* **2011**, *123*, 12808 – 12812; *Angew. Chem. Int. Ed.* **2011**, *50*, 12600 – 12604.
[6] a) J. J. Concepcion, J. W. Jurss, M. K. Brennaman, P. G. Hoertz, A. O. v. T. Patrocinio, N. Y. Murakami Iha, J. L. Templeton, T. J. Meyer, *Acc. Chem. Res.* **2009**, *42*, 1954 – 1965; b) D. J. Wasylenko, C. Ganesamoorthy, M. A. Henderson, B. D. Koivisto, H. D. Osthoff, C. P. Berlinguette, *J. Am. Chem. Soc.* **2010**, *132*, 16094 – 16106; c) D. E. Polyansky, J. T. Muckerman, J. Rochford, R. Zong, R. P. Thummel, E. Fujita, *J. Am. Chem. Soc.* **2011**, *133*, 14649 – 14665; d) D. G. H. Hetterscheid, J. N. H. Reek, *Angew. Chem.* **2012**, *124*, 9878 – 9885; *Angew. Chem. Int. Ed.* **2012**, *51*, 9740 – 9747; e) D. J. Wasylenko, R. D. Palmer, C. P. Berlinguette, *Chem. Commun.* **2013**, *49*, 218 – 227.
[7] J. J. Concepcion, M.-K. Tsai, J. T. Muckerman, T. J. Meyer, *J. Am. Chem. Soc.* **2010**, *132*, 1545 – 1557.
[8] J. Concepcion, J. Jurss, P. Hoertz, T. Meyer, *Angew. Chem.* **2009**, *121*, 9637 – 9640; *Angew. Chem. Int. Ed.* **2009**, *48*, 9473 – 9476.
[9] S. Maji, I. López, F. Bozoglian, J. Benet-Buchholz, A. Llobet, *Inorg. Chem.* **2013**, *52*, 3591 – 3593.
[10] a) T. W. Welch, S. A. Ciftan, P. S. White, H. H. Thorp, *Inorg. Chem.* **1997**, *36*, 4812 – 4821; b) C. M. Che, T. F. Lai, K. Y. Wong, *Inorg. Chem.* **1987**, *26*, 2289 – 2299; c) W.-C. Cheng, W.-Y. Yu, K.-K. Cheung, C.-M. Che, *J. Chem. Soc. Dalton Trans.* **1994**, 57 – 62; d) C. M. Che, W. T. Tang, W. T. Wong, T. F. Lai, *J. Am. Chem. Soc.* **1989**, *111*, 9048 – 9056; e) T. Kojima, K. Nakayama, K. Ikemura, T. Ogura, S. Fukuzumi, *J. Am. Chem. Soc.* **2011**, *133*, 11692 – 11700; f) W.-C. Cheng, W.-Y. Yu, J. Zhu, K.-K. Cheung, S.-M. Peng, C.-K. Poon, C.-M. Che, *Inorg. Chim. Acta* **1996**, *242*, 105 – 113; g) K. Aoyagi, Y. Yukawa, K. Shimizu, M. Mukaida, T. Takeuchi, H. Kakihana, *Bull. Chem. Soc. Jpn.* **1986**, *59*, 1493 – 1499.
[11] a) T. R. Weaver, T. J. Meyer, S. A. Adeyemi, G. M. Brown, R. P. Eckberg, W. E. Hatfield, E. C. Johnson, R. W. Murray, D. Untereker, *J. Am. Chem. Soc.* **1975**, *97*, 3039 – 3048; b) A. Llobet, M. E. Curry, H. T. Evans, T. J. Meyer, *Inorg. Chem.* **1989**, *28*, 3131 – 3137; c) R. Schneider, T. Weyhermueller, K. Wieghardt, B. Nuber, *Inorg. Chem.* **1993**, *32*, 4925 – 4934.
[12] a) B. A. Moyer, T. J. Meyer, *Inorg. Chem.* **1981**, *20*, 436 – 444; b) C. L. Bailey, R. S. Drago, *J. Chem. Soc. Chem. Commun.* **1987**, 179 – 180; c) D. Chatterjee, *Inorg. Chim. Acta* **2008**, *361*, 2177 – 2182; d) W. P. Griffith in *Catalysis by Metal Complexes, Vol. 34* (Eds.: C. Bianchini, D. J. Cole-Hamilton, P. W. N. M. van Leeuwen), Springer, Heidelberg, **2011**.
[13] J. W. Jurss, J. J. Concepcion, J. M. Butler, K. M. Omberg, L. M. Baraldo, D. G. Thompson, E. L. Lebeau, B. Hornstein, J. R. Schoonover, H. Jude, J. D. Thompson, D. M. Dattelbaum, R. C. Rocha, J. L. Templeton, T. J. Meyer, *Inorg. Chem.* **2012**, *51*, 1345 – 1358.
[14] a) Y. Zhao, D. G. Truhlar, *J. Chem. Phys.* **2006**, *125*, 194101; b) Y. Zhao, D. G. Truhlar, *Acc. Chem. Res.* **2008**, *41*, 157; c) Y. Zhao, D. G. Truhlar, *Theor. Chem. Acc.* **2008**, *120*, 215.
[15] The TOFs were calculated by transforming the current intensity at 1.6 V vs. SSCE into mols of oxygen produced per second: I/(4 electrons × 96485), and dividing this value by the amount of catalyst next to the electrode surface, which was determined on the basis of the area under the anodic wave of the IV,IV/III,III couple in the case of $\mathbf{1}^{4+}$ or the III/II couple in the case of $\mathbf{4}^{2+}$.
[16] M. D. Kärkäs, T. Åkermark, H. Chen, J. Sun, B. Åkermark, *Angew. Chem.* **2013**, *125*, 4283 – 4287; *Angew. Chem. Int. Ed.* **2013**, *52*, 4189 – 4193.
[17] a) S. A. Adeyemi, A. Dovletoglou, A. R. Guadalupe, T. J. Meyer, *Inorg. Chem.* **1992**, *31*, 1375 – 1383; b) J. M. Mayer, *Comments Inorg. Chem.* **1988**, *8*, 125 – 135.
[18] a) F. Bozoglian, S. Romain, M. Z. Ertem, T. K. Todorova, C. Sens, J. Mola, M. Rodriguez, I. Romero, J. Benet-Buchholz, X. Fontrodona, C. J. Cramer, L. Gagliardi, A. Llobet, *J. Am. Chem. Soc.* **2009**, *131*, 15176 – 15187; b) X. Sala, M. Z. Ertem, L. Vigara, T. K. Todorova, W. Chen, R. C. Rocha, F. Aquilante, C. J. Cramer, L. Gagliardi, A. Llobet, *Angew. Chem.* **2010**, *122*, 7911 – 7913; *Angew. Chem. Int. Ed.* **2010**, *49*, 7745 – 7747.

